

# A synthetic aperture interferometric radiometer test at X-band for potential improvements at W-band

Yassine Aouial, Olivier Lafond, Stéphane Méric and Mohamed Himdi

Institute of Electronic and Telecommunication of Rennes

Rennes, France

[yassine.aouial@univ-rennes1.fr](mailto:yassine.aouial@univ-rennes1.fr), [olivier.lafond@univ-rennes1.fr](mailto:olivier.lafond@univ-rennes1.fr),  
[stephane.meric@insa-rennes.fr](mailto:stephane.meric@insa-rennes.fr), [mohamed.himdi@univ-rennes1.fr](mailto:mohamed.himdi@univ-rennes1.fr)

**Abstract** — The broad topic of the presented paper consists in the research on novel methods in the field of microwave imaging, in particular the so-called passive microwave / millimeter-wave imaging, which is also referred to radiometric imaging. This study focuses on proximity range applications such as concealed objects detection, human body screening, etc. The aim is to design a low cost and compact fully electronic passive imaging system suitable for short-range 2D imaging applications, and study the necessary devices for the implementation of a complete demonstrator. In this study, a new approach based on the use of a switch sub-matrix strategy has been adapted into a complete antenna system at X band. The main objective of this prototype is to validate this approach experimentally. Image quality is examined by using the interferometric aperture synthesis technique and G-matrix calibration imaging algorithms. The spatial resolution is measured using the emission from noise source and compared with theory.

**Keywords**—component; formatting; style; styling; insert (key words)

## I. INTRODUCTION

In the recent years, the application of passive imaging has gained increasing interest [1]. For proximity range applications as concealed weapons detection, millimeter wave imaging systems are suggested as an effective tool to detect explosives, hidden and other dangerous objects and contraband [2]. In the literature, passive imaging systems are mainly based on three types of radiometers: real aperture (RA) radiometer [3], 1-D synthetic aperture (SA) (1D-SA) radiometer [4], and 2-D SA (2D-SA) radiometer [5]. The first and the second rely on a mechanical scanning system in order to acquire a 2-D image. While the 2-D SA is based on an electronic scanning system.

Selecting one of the systems mentioned earlier represents a trade off between hardware complexity and imaging performance. The 2-D SA principle could reduce the volume of the imaging system and improve its performances [6]. In fact, by eliminating focusing lenses, mirrors and mechanical scanners, the imaging system volume can then be reduced. In addition, the image quality can be enhanced by many efficient processing [7] which permit to achieve a high spatial resolution and to calibrate the errors of the system. Motivation for the development of 2-D SA imagers is that they have the potential to be constructed in a planar format and thereby be integrated into existing wall surfaces for security purposes.

The most of imaging systems using aperture synthesis principles are based on the conventional mutli-channels approach, which depends mainly on the number of receivers. However, a new low-cost approach has been proposed [8] that based on the switching strategy. Therefore, the work presented here focuses on the development of a system based on this approach. The working frequency is around 11 GHz. After detailing the principle of the 2-D SA imaging by the switching strategy, we describe the various modules of the system and the imaging procedure and characteristics and finally we give possible performance of the system from measurements of the target.

## II. APERTURE SYNTHESIS IMAGING BY THE SWITCH SUB-MATRIX STRATEGY

### A. Imaging principle by Aperture Synthesis

The general theory concerning aperture synthesis for passive imaging is published in [9]. Its basic strength enables large collecting areas to be synthesised using physically much smaller collecting antennas and receivers to deliver high spatial resolution. The aperture synthesis imager measures the complex correlation between signals collected by two spatially separated antennas ( $k$  and  $l$ ) that have overlapping fields of view, yielding samples of visibility function  $V$  of the brightness temperature  $T_B$  of the scene under observation. Fig.1 shows the schematic of a two dimensional geometric arrangement for the 2D-SA imaging. In an ideal case, far field situation, the relationship between visibility and brightness temperature is given by:

$$V_{kl}(u_{kl}, v_{kl}) = \frac{1}{\sqrt{\Omega_k \Omega_l}} \iint_{\xi^2 + \eta^2 \leq 1} \frac{T_B(\xi, \eta) - T_r}{\sqrt{1 - \xi^2 - \eta^2}} F_k(\xi, \eta) \overline{F_l(\xi, \eta)} \times \tilde{r}_{kl} \left( \frac{u_{kl}\xi + v_{kl}\eta}{f_0} \right) \exp^{-j2\pi(u_{kl}\xi + v_{kl}\eta)} d\xi d\eta \quad (1)$$

where  $(u_{kl}, v_{kl}) = (x_k - x_l, y_k - y_l) / \lambda_0$  denotes the spatial frequency (Baseline) that depends on the antenna position  $(x, y)$  difference,  $(\xi, \eta) = (\sin \theta \cos \varphi, \sin \theta \sin \varphi)$  is the direction cosines defined with respect to the x- and y-axis,  $T_r$  is the physical temperature of the receivers,  $\Omega$  is the solid angle of the antennas and  $F$  denotes the normalized antenna voltage patterns. The function  $\tilde{r}_{kl}()$  is the so-called fringe-washing

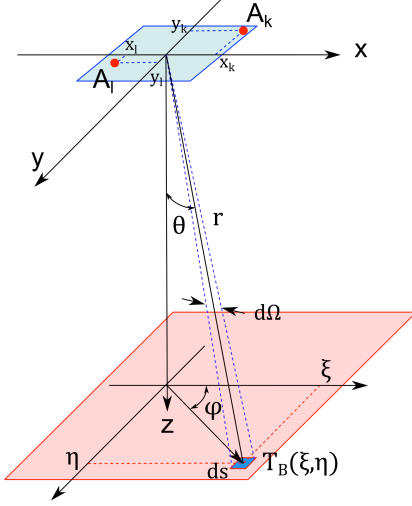


Fig. 1. Schematic of two-dimensional geometric arrangement for the aperture synthesis imaging.

function that depends on the frequency response of the pair of elements whose signals being correlated. The image of the brightness temperature of the scene can be found then via a reverse process [7].

#### B. The Switching Sub-matrix Strategy

The most of imaging systems using aperture synthesis principles are based on the conventional multi-channels approach. However, a system that the subject of high spatial resolution requires a hundred of antennas and receiver channels and this approach might not be a low-cost concept. Therefore, a new approach has been proposed [8] that based on the switching strategy. This strategy is of interest in an imaging system as they sample all spatial frequencies across an aperture with the minimum number of receivers in order to improve the cost-performance ratio compared to a conventional system. The concept of using a 2D imaging interferometer by two-dimensional approach sub-matrices Switch is detailed in [8]. The principle is based on using only two receiver channels associated to an antenna array through two independent sub-matrices of switches. To implement this approach, an optimization process to find the optimal configuration based on the size of the array has also been proposed [10]. For the size of 7x7 elements, Fig. 2 shows the optimum array found with a minimum number of antennas. This optimum array provides full rectangular spatial frequency coverage and therefore the same spatial resolution in contrast to the fully filled configuration. This structure shows several advantages in terms of resolution, complexity and cost, which have satisfy the requirements for the considered demonstrator.

### III. SYSTEM ARCHITECTURE AND CHARACTERISTICS

To investigate how well 2-D SA passive imager function, a proof of concept demonstrator at X-band has been designed, built and characterised. The RF center frequency is 11 GHz and the IF center frequency is 50 MHz with a 50 MHz system bandwidth. The measurement setup consists of the correlation between all enabling antennas. A total aperture synthesis is obtained by sequentially switching antenna elements in all

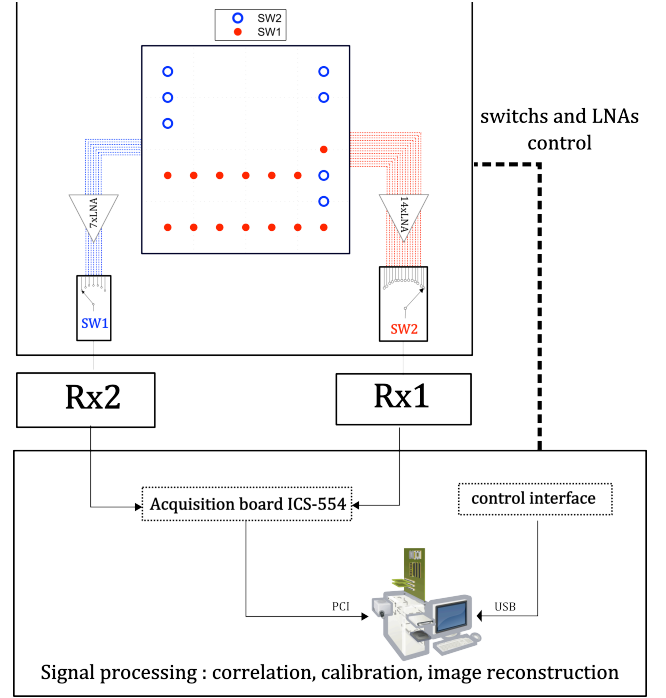


Fig. 2. System Block diagram at X-band

possible, required pairs of positions and measuring the corresponding samples of the visibility function.

#### A. System Block diagram

The system is composed of three modules that provide the necessary system hardware and software functionalities as shown in Fig. 2: antenna and front-end module, receiver module and signal processing module. The antenna and front-end module is composed of a 21 patch antennas placed in a sparse array, 21 LNAs and 8 MMIC single-pole multiple-throw switches (SP4T). Consequently, using multilayer manufacturing technology as shown in Fig. 3 can easily integrate the switch sub-matrix. The top layer is used for antennas and the bottom layer for the front-end. The least spacing between antennas is  $0.75\lambda_0$ , and the maximum spacing is  $3.5\lambda_0$ . The antenna elements receive signals in the horizontal polarization mode, and the gain is over 6 dB. For the measured H-plane radiation pattern, the half-power beamwidth (HPBW) is about  $75^\circ$ . The measured E-plane radiation patterns show that the HPBW for one antenna element is about  $90^\circ$ .

For the receiver module (Rx1 and Rx2), the receiver circuitry follows a heterodyne-circuit concept with double-frequency down conversion. The received signal is down converted to the first intermediate frequency (IF), filtered and amplified further to provide a power level that is adequate for the following analog-to-digital (A/D) conversion. The final down conversion and demodulation to a baseband are performed by the digital electronic circuitry after sampling of the analog signal at 100-MHz sampling frequency.

The signals are sampled and digitized by the A/D acquisition board and processed by a computer for image reconstruction. Since the amplitude mismatch, phase shift, and mutual coupling in the antenna array will introduce amplitude

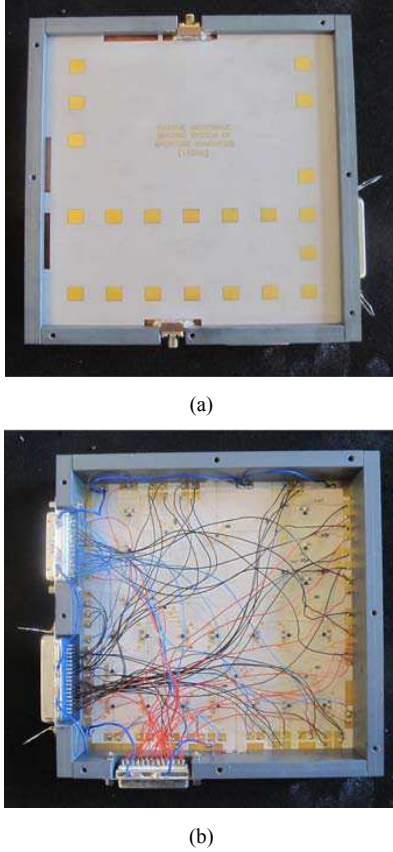


Fig. 3. The 11 GHz aperture synthesis imager. (a) Antenna module (b) front-end module

and phase errors, the calibration algorithm must be considered also. The complete system is driven from a PC and uses Matlab to process data, running the image reconstruction algorithms to create still images and videos.

#### B. System calibration and image reconstruction

The calibration algorithm for an aperture synthesis radiometer had been described in [11]. Due to system imperfections, such as antenna errors, channel errors, each antenna radiation pattern and the frequency response of each receiver will be influenced, and then the brightness temperature in the field of view (FOV) is affected by the system.

In the most general sense this calibration can be represented by matrix operations on vectors. The Eq. 1 can also be written in terms of the response of the imager system to the scene, and this is given by Eq. 2, where vector  $V_n$  is the visibilities of length  $n$  and the vector  $T_B$  is the brightness temperature from  $m$  pixels in the scene and  $G_{n,m}$  is the response matrix. Inversion of this equation gives the temperature at each pixel for a given visibilities, where  $G'_{m,n}$  is the calibration matrix, as in Eq. 3. The calibration matrix, a large matrix of  $m \times n$  elements, can be found by inversion of the response matrix. The response matrix is found by measuring farfield radiation pattern in the phase center of each antenna (i.e Fig. 4) and the frequency response of each receiver. This method of calibration is similar to passing a source through all the pixels in the field of view and recording the responses  $V_n$ .

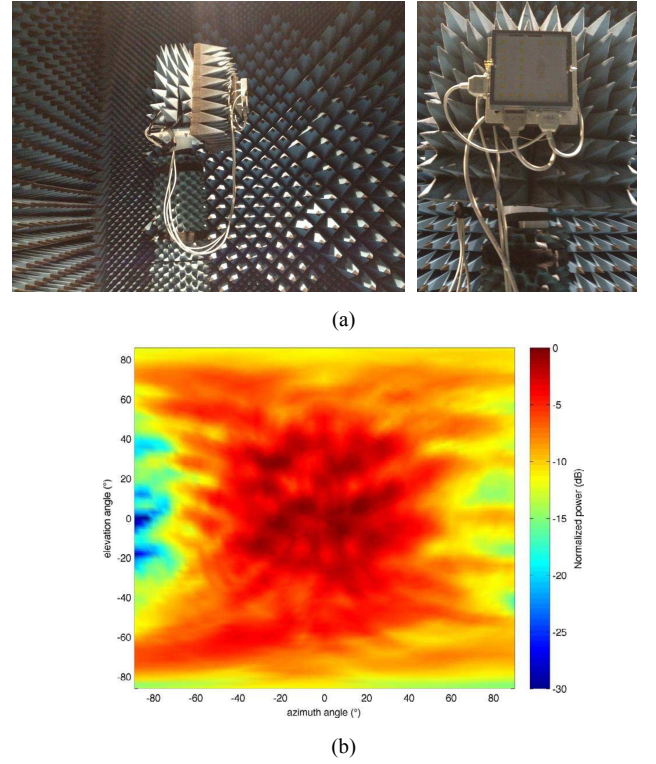


Fig. 4. (a) Farfield radiation pattern measurement setup (b) farfield radiation pattern at 11GHz of one antenna in azimuth and elevation axis.

$$V_n = G_{n,m} T_m \quad (2)$$

$$\hat{T}_m = G'_{m,n} V_n \quad \text{where} \quad G'_{m,n} = G_{n,m}^H \left( G_{n,m} G_{n,m}^H \right)^{-1} \quad (3)$$

#### IV. EXPERIMENTS AND RESULTS

In order to demonstrate the possibility of using the sub-matrices approach in a passive imaging radiometer system, a series of experiments was conducted. These experiments include a noise source measurement experiment at X-band. Therefore, a noise source was placed at 2 m from the system. The output power of the noise source is set high that the thermal noise from the background. Fig. 5.a shows the prototype of the experiment in anechoic chamber. After system calibration, the system response of the point source in two directions can be seen in Fig. 5. The estimated incident direction of the noise source is precise, and the background brightness temperature is slightly stable.

Concerning system performances, the measured angular resolution is  $6.5^\circ$ . Theoretically, this resolution value is equal to  $6.3^\circ$ . Consequently, the measured and theoretical angular resolutions are in good agreement. The measurement of the radiometric sensitivity of the X-band aperture synthesis imager was calculated by using relationship [6]:

$$\Delta T = \frac{T_B + T_R}{\sqrt{B\tau}} \left( \frac{D_{syn}}{\lambda_0} \right)^2 \left( \frac{\Omega_{FOV}}{N} \right) \quad (4)$$



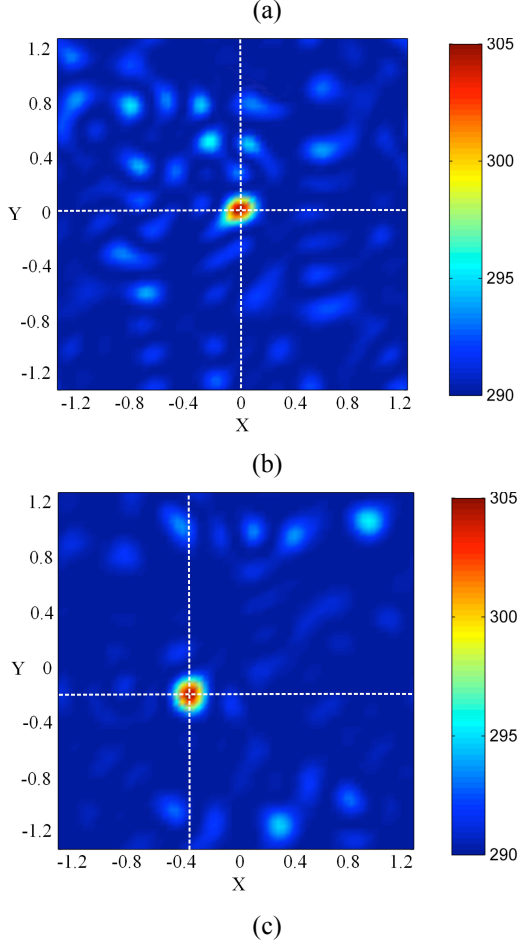
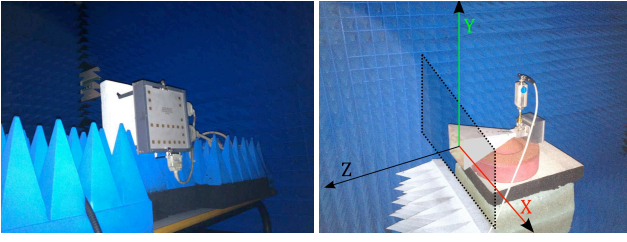


Fig. 5. (a) Measurement setup using a noise signal as point source. (b) and (c) reconstructed image of a noise source located at the center of the scene and at  $(x, y) = (-0.4, -0.2)$

where  $B$  is the bandwidth of the receiver,  $\tau$  is the equivalent integration time,  $N$  is the number of antennas,  $D_{syn}$  is the diameter of the synthetic aperture,  $\Omega_{FOV}$  is the FOV solid angle,  $T_B$  is the brightness temperature of the scene,  $T_R$  is the effective receiver noise temperature. For this demonstrator, the equivalent integration time is about 10 ms and the bandwidth is about 50 MHz. The sensitivity of the system is less than 9 K, when  $T_B$  is 300 K. The radiometric sensitivity describes the capacity of the system to distinguish among small scene contrasts in the image. Actually, the sensitivity value of the system is not good to detect concealed objects with an apparent temperature similar to that of the background. The principal objectives of the project are to develop a demonstrator having a low-cost and real-time imaging capability. Therefore, follow on

demonstrators require higher specifications (sensitivity and resolution) of the system and a choice of the optimal frequency (W-band) for the scenario.

## V. CONCLUSION

In this paper, based on research on a low-cost fully electronic passive imaging system, the concept of using the switching sub-matrix strategy to develop a low cost system for proximity range applications has been presented. Obviously, this approach has important benefits in terms of cost and system compactness. The experiment result demonstrates the angular resolution and sensitivity of the system. For the further work, the future demonstrator will illustrate how a 2-D SA imaging architecture delivers real-time imagery with a sensitivity to detect threats of interest for security scanning portals. This will possibly in W-band for the optimum radiometric contrast [12].

## REFERENCES

- [1] R. N. Anderton, R. Appleby, J. E. Beale, P. R. Coward, and S. Price, "Security scanning at 94 GHz," in *Proc. SPIE*, R. Appleby and D. A. Wikner, Eds., 2006, vol. 6211, no. 1, pp. 62110C-1–62110C-7.
- [2] R. Appleby and R. N. Anderton, "Millimeter-wave and submillimeterwave imaging for security and surveillance," *Proc. IEEE*, vol. 95, no. 8, pp. 1683–1690, Aug. 2007.
- [3] D. Notel, J. Huck, S. Neubert, S. Wirtz, and A. Tessmann, "A compact mmW imaging radiometer for concealed weapon detection," in *Proc. Joint 32nd Int. Conf./15th Int. Conf. IRMMW-THz*, 2007, pp. 269–270.
- [4] D. Le Vine, A. Griffiths, C. Swift, and T. Jackson, "ESTAR: A synthetic aperture microwave radiometer for remote sensing applications," *Proc. IEEE*, vol. 82, no. 12, pp. 1787–1801, Dec. 1994.
- [5] N. A. Salmon, R. Macpherson, A. Harvey, P. Hall, S. Hayward, P. Wilkinson, and C. Taylor, "First video rate imagery from a 32-channel 22-ghz aperture synthesis passive millimetre wave imager," K. A. Krapels, N. A. Salmon, and E. Jacobs, Eds., vol. 8188, no. 1. SPIE, 2011, p. 818805.
- [6] N. Salmon, J. Beale, J. Parkinson, S. Hayward, P. Hall, R. Macpherson, R. Lewis, and A. Harvey, "Digital beam-forming for passive millimetre wave security imaging," *IET Seminar Digests*, vol. 2007, no. 11961, pp. 181–181, 2007.
- [7] E. Anterrieu, "A resolving matrix approach for synthetic aperture imaging radiometers," *IEEE Transactions on Geoscience and Remote Sensing*, vol. 42, no. 8, pp. 1649 – 1656, aug. 2004
- [8] Y. Aouial, S. Méric, O. Lafond, and M. Himdi, "Synthesis of Sparse Planar Arrays for Passive Imaging Systems Based on Switch Submatrix," *IEEE Geoscience and Remote Sensing Letters*, (2012), 1007–1011.
- [9] C. Ruf, C. Swift, A. Tanner, and D. Le Vine, "Interferometric synthetic aperture microwave radiometry for the remote sensing of the earth," *IEEE Transactions on Geoscience and Remote Sensing*, vol. 26, no. 5, pp. 597–611, Sep. 1988
- [10] Y. Aouial, S. Méric, O. Lafond, and M. Himdi, "Passive millimeter wave imaging : 2D sparse array optimization for low cost system architecture," *Proceedings of the 6th European Conference on Antennas and Propagation (EUCAP)*, march 2012, pp. 3421–3425
- [11] I. Corbella, et al, "MIRAS End-to-End Calibration: Application to SMOS L1 Processor", *IEEE Transactions on Geoscience and Remote Sensing*, Vol. 43, No. 5, May, (2005)
- [12] E. Nova, J. Romeu, F. Torres, M. Pablos, J. M. Riera, A. Broquetas, L. Jofre, "Radiometric and Spatial Resolution Constraints in Millimeter-Wave Close-Range Passive Screener Systems," *Geoscience and Remote Sensing, IEEE Transactions on*, vol. PP, no. 99, pp. 1–10